A study of the $^{16}\mathbf{O}(e,e'p)$ reaction at deep missing energies

N. Liyanage,[17] B. D. Anderson,[13] K. A. Aniol,[2] L. Auerbach,[29] F. T. Baker,[7] J. Berthot,[1] W. Bertozzi,[17] P. -Y. Bertin,[1] L. Bimbot,[22] W. U. Boeglin,[5] E. J. Brash,[24] V. Breton,[1] H. Breuer,[16] E. Burtin,[26] J. R. Calarco,[18] L. Cardman,[30] G. D. Cates,[23] C. Cavata,[26] C. C. Chang,[16] J. -P. Chen,[30] E. Cisbani,[12] D. S. Dale,[14] R. De Leo,[10] A. Deur,[1] B. Diederich,[21] P. Djawotho,[33] J. Domingo,[30] B. Doyle,[14] J. -E. Ducret,[26] M. B. Epstein,[2] L. A. Ewell,[16] J. M. Finn,[33] K. G. Fissum,[17] H. Fonvieille,[1] B. Frois,[26] S. Frullani,[12] J. Gao,[17] F. Garibaldi,[12] A. Gasparian,[8,14] S. Gilad,[17] R. Gilman,[25,30] A. Glamazdin,[15] C. Glashausser,[25] J. Gomez,[30] V. Gorbenko,[15] T. Gorringe,[14] K. Griffioen,[33] F. W. Hersman,[18] R. Holmes,[28] M. Holtrop,[18] N. d'Hose,[26] C. Howell,[4] G. M. Huber,[24] C. E. Hyde-Wright,[21] M. Iodice,[12] C. W. de Jager,[30] S. Jaminion,[1] M. K. Jones,[33] K. Joo,[32] C. Jutier,[1,21] W. Kahl,[28] S. Kato,[34] J. J. Kelly,[16] S. Kerhoas,[26] M. Khandaker,[19] M. Khayat,[13] K. Kino,[31] W. Korsch,[14] L. Kramer,[5] K. S. Kumar,[23] G. Kumbartzki,[25] G. Laveissière,[1] A. Leone,[11] J. J. LeRose,[30] L. Levchuk,[15] M. Liang,[30] R. A. Lindgren,[32] G. J. Lolos,[24] R. W. Lourie,[27] R. Madey,[8,13,30] K. Maeda,[31] S. Malov,[25] D. M. Manley,[13] D. J. Margaziotis[2] P. Markowitz,[5] J. Martino,[26] J. S. McCarthy,[32] K. McCormick,[21] J. McIntyre,[25] R. L. J. van der Meer,[24] Z. -E. Meziani,[29] R. Michaels,[30] J. Mougey,[3] S. Nanda,[30] D. Neyret,[26] E. A. J. M. Offermann,[30] Z. Papandreou,[24] C. F. Perdrisat,[33] R. Perrino,[11] G. G. Petratos,[13] S. Platchkov,[26] R. Pomatsalyuk,[15] D. L. Prout,[13] V. A. Punjabi,[19] T. Pussieux,[26] G. Quéméner,[33] R. D. Ransome,[25] O. Ravel,[1] Y. Roblin,[1] R. Roche,[6] D. Rowntree,[17] G.A. Rutledge,[33] P. M. Rutt,[30] A. Saha,[30] T. Saito,[31] A. J. Sarty,[6] A. Serdarevic-Offermann,[24] T. P. Smith,[18] A. Soldi,[20] P. Sorokin,[15] P. Souder,[28] R. Suleiman,[13] J. A. Templon,[7] T. Terasawa,[31] L. Todor,[21] H. Tsubota,[31] H. Ueno,[34] P. E. Ulmer,[21] G.M. Urciuoli,[12] P. Vernin,[26] S. van Verst,[17] B. Vlahovic,[20] H. Voskanyan,[35] J. W. Watson,[13] L. B. Weinstein,[21] K. Wijesooriya,[33] R. Wilson,[9] B. Wojtsekhowski,[30] D. G. Zainea,[24] V. Zeps,[14] J. Zhao,[17] Z. -L. Zhou[17]

(The Jefferson Lab Hall A Collaboration)

[1] *Université Blaise Pascal/IN2P3, F-63177 Aubière, France*
[2] *California State University, Los Angeles, California, 90032, USA*
[3] *Institut des Sciences Nucléaires, F-38026 Grenoble, France*
[4] *Duke University, Durham, North Carolina, 27706, USA*
[5] *Florida International University, Miami, Florida, 33199, USA*
[6] *Florida State University, Tallahassee, Florida, 32306, USA*
[7] *University of Georgia, Athens, Georgia, 30602, USA*
[8] *Hampton University, Hampton, Virginia, 23668, USA*
[9] *Harvard University, Cambridge, Massachusetts, 02138, USA*
[10] *INFN, Sezione di Bari and University of Bari, I-70126 Bari, Italy*
[11] *INFN, Sezione di Lecce, I-73100 Lecce, Italy*
[12] *INFN, Sezione Sanitá and Istituto Superiore di Sanitá, Laboratorio di Fisica, I-00161 Rome, Italy*
[13] *Kent State University, Kent, Ohio, 44242, USA*
[14] *University of Kentucky, Lexington, Kentucky, 40506, USA*
[15] *Kharkov Institute of Physics and Technology, Kharkov 310108, Ukraine*
[16] *University of Maryland, College Park, Maryland, 20742, USA*
[17] *Massachusetts Institute of Technology, Cambridge, Massachusetts, 02139, USA*
[18] *University of New Hampshire, Durham, New Hampshire, 03824, USA*
[19] *Norfolk State University, Norfolk, Virginia, 23504, USA*
[20] *North Carolina Central University, Durham, North Carolina, 27707, USA*
[21] *Old Dominion University, Norfolk, Virginia, 23529, USA*
[22] *Institut de Physique Nucléaire, F-91406 Orsay, France*
[23] *Princeton University, Princeton, New Jersey, 08544, USA*
[24] *University of Regina, Regina, Saskatchewan, Canada, S4S 0A2*
[25] *Rutgers, The State University of New Jersey, Piscataway, New Jersey, 08854, USA*
[26] *CEA Saclay, F-91191 Gif-sur-Yvette, France*
[27] *State University of New York at Stony Brook, Stony Brook, New York, 11794, USA*
[28] *Syracuse University, Syracuse, New York, 13244, USA*
[29] *Temple University, Philadelphia, Pennsylvania, 19122, USA*
[30] *Thomas Jefferson National Accelerator Facility, Newport News, Virginia, 23606, USA*
[31] *Tohoku University, Sendai 980, Japan*
[32] *University of Virginia, Charlottesville, Virginia, 22901, USA*
[33] *College of William and Mary, Williamsburg, Virginia, 23187, USA*
[34] *Yamagata University, Yamagata 990, Japan*
[35] *Yerevan Physics Institute, Yerevan 375036, Armenia*

(June 26, 2000)

We measured ^{16}O$(e,e'p)$ cross sections and response functions (R_L, R_T and R_{LT}) in quasielastic kinematics at $Q^2 = 0.8$ (GeV/c)^2 and $\omega = 439$ MeV for missing energies $25 \leq E_{\rm miss} \leq 120$ MeV at various missing momenta $P_{\rm miss} \leq 340$ MeV/c. For $25 < E_{\rm miss} < 50$ MeV and $P_{\rm miss} \approx 60$ MeV/c the reaction is dominated by single-nucleon knockout from the $1s_{1/2}$-state. At larger $P_{\rm miss}$ the single-particle aspects are increasingly masked by more complicated states and processes. For $E_{\rm miss} > 60$ MeV and $P_{\rm miss} > 100$ MeV/c, the cross section is relatively constant and appears to be due to two-nucleon knockout.

PACS numbers: 25.30.Fj, 27.20.+n

The $(e,e'p)$ reaction in quasielastic kinematics ($\omega \approx Q^2/2m_p$)[1] has long been a useful tool for the study of nuclear structure. $(e,e'p)$ cross section measurements have provided both a wealth of information on the wave function of protons inside the nucleus and stringent tests of nuclear theories. Response function measurements have provided detailed information about the different reaction mechanisms contributing to the cross section.

In the first Born approximation, the unpolarized $(e,e'p)$ cross section can be expressed as [1]

$$\frac{d^6\sigma}{d\Omega_e d\Omega_p d\omega dE_p} = \frac{p_p E_p}{(2\pi)^3}\sigma_{\rm Mott}(V_L R_L + V_T R_T + V_{LT} R_{LT}\cos\phi + V_{TT} R_{TT}\cos 2\phi) \qquad (1)$$

where V_L, V_T, V_{LT}, and V_{TT} are known kinematic factors and $\sigma_{\rm Mott}$ is the Mott cross section. The four independent response functions R_L (longitudinal), R_T (transverse), R_{LT} (longitudinal-transverse), and R_{TT} (transverse-transverse) contain all the information that can be extracted from the hadronic system using the $(e,e'p)$ reaction. One can separate the response functions by measuring the cross section at fixed Q^2, ω and θ_{pq} while varying θ_e (which varies V_T) and ϕ.

Originally, the quasielastic cross section was attributed entirely to single-particle knockout from the valence states of the nucleus. However, a series of ^{12}C$(e,e'p)$ experiments performed at MIT-Bates [2–5] measured much larger cross sections at high missing energy than were expected by single-particle knockout models. ^{12}C$(e,e'p)$ response function data reported by Ulmer *et al.* [2] show a substantial increase in the transverse-longitudinal difference, $(S_T - S_L)$,[2] above the two-nucleon emission threshold. Similar R_T/R_L enhancement has also been observed by Lanen *et al.* for ^{6}Li [8], by van der Steenhoven *et al.* for ^{12}C [9] and, more recently, by Dutta *et al.* for ^{12}C, ^{56}C, and ^{197}Au at $Q^2 = 0.6$ (GeV/c)^2 [10]. These findings suggest that a significant part of the cross section at large missing energies is due to two-body and multi-body processes.

There have been several theoretical attempts [11–13] to explain the continuum strength using two-body knockout models and final-state interactions, but no single model can explain all the data. It has also been suggested that short-range and tensor correlations could play a major role in populating the high-$E_{\rm miss}$ continuum. Müther *et al.* [14] have shown that these effects shift strength from conventional quasi-hole states to high-$E_{\rm miss}$, high-$P_{\rm miss}$ channels.

In this experiment [15], we studied the ^{16}O$(e,e'p)$ reaction in the quasielastic region at $Q^2 = 0.8$ (GeV/c)^2 and $\omega = 439$ MeV. We extracted the R_L, R_T, and R_{LT} response functions from cross sections measured at several beam energies and electron angles for $E_{\rm miss} \leq 60$ MeV and $P_{\rm miss} \leq 340$ MeV/c. This was the first Jefferson Lab Hall A experiment and the first response function separation on a complex nucleus at large $E_{\rm miss}$ and $P_{\rm miss}$. This paper reports the results for $E_{\rm miss} > 25$ MeV.

We scattered the $\sim 70\mu$A continuous incident electron beam from a waterfall target [16] with three foils, each ~ 130 mg/cm^2 thick. We detected the scattered electrons and knocked-out protons in the two High Resolution Spectrometers (HRS$_e$ and HRS$_h$). The details of the Hall A experimental setup are given in [17,18].

We measured the ^{16}O$(e,e'p)$ cross section at three beam energies keeping $|\vec{q}|$ and ω fixed in order to separate response functions and understand systematic uncertainties (Table I shows the experimental kinematics).

The accuracy of a response function separation depends on precisely matching the values of $|\vec{q}|$ and ω for different kinematic settings. In order to match $|\vec{q}|$, we measured H(e,ep) (also using the waterfall target) with a pin-hole collimator in front of the HRS$_e$. The momentum of the detected protons was thus equal to $\vec{q}$. We determined the H(e,ep) momentum peak to $\frac{\delta p}{p} = 1.5 \times 10^{-4}$, allowing us to match $|\vec{q}|$ to 1.5×10^{-4} between the different kinematic settings. Throughout the experiment, H(e,e) data, measured simultaneously with ^{16}O$(e,e'p)$,

[1] The kinematical quantities are as follows: the electron scattered at angle θ_e transfers momentum $\vec{q}$ and energy ω with $Q^2 = \vec{q}^{\,2} - \omega^2$. The ejected proton has mass m_p, momentum $\vec{p}_p$, energy E_p, and kinetic energy T_p. The cross section is typically measured as a function of missing energy $E_{\rm miss} = \omega - T_p - T_{recoil}$ and missing momentum $P_{\rm miss} = |\vec{q} - \vec{p}_p|$. The angle between the ejected proton and virtual photon is θ_{pq} and the out-of-plane angle is ϕ. $\theta_{pq} > 0$ corresponds to $\phi = 180°$ and $\theta_p > \theta_q$. $\theta_{pq} < 0$ corresponds to $\phi = 0°$.

[2] $S_X = \frac{\sigma_M V_X R_X}{\sigma_X^{ep}}$, where X ϵ $\{T, L\}$, and σ_X^{ep} is calculated from the off-shell ep cross section obtained using deForest's cc1 prescription [6,7].

provided a continuous monitor of both luminosity and beam energy.

The radiative corrections to the measured cross sections were performed using the code RADCOR [18,19], which unfolds the radiative tails in $(E_{\rm miss}, P_{\rm miss})$ space. For the $\theta_{pq} = 0^\circ$ kinematic setting, the H(e,ep) peak and its associated radiative tail were present in the coincidence phase space for ^{16}O. To remove H(e,ep) events, we cut out all events with $P_{\rm miss} < 45$ MeV/c and $|E_{\rm miss} - P_{\rm miss}| \leq 10$ MeV.

At $\theta_{pq} = \pm 8^\circ$, R_{LT} extracted independently at beam energies of 1.643 GeV and 2.442 GeV agree well within statistical uncertainties. This indicates that the systematic uncertainties are smaller than the statistical uncertainties.

Figure 1 shows our measured cross sections as a function of missing energy at $E_{\rm beam} = 2.4$ GeV for various proton angles, $2.5^\circ \leq \theta_{pq} \leq 20^\circ$. The average missing momentum $\langle P_{\rm miss} \rangle$ increases with θ_{pq} from 50 MeV/c to 340 MeV/c. There are three main features: two sharp peaks at $E_{\rm miss} < 20$ MeV, a broad peak centered at $E_{\rm miss} = 40$ MeV, and a flat cross section at larger $E_{\rm miss}$. The prominent peaks at 12 and 18 MeV are due to $1p$-shell proton knockout and are described in [20]. At the lowest missing momentum, $P_{\rm miss} \approx 50$ MeV/c, there is a wide peak centered at $E_{\rm miss} \sim 40$ MeV due predominantly to knockout of protons from the $1s_{1/2}$-state. This peak is less prominent at $P_{\rm miss} \approx 145$ MeV/c and has vanished beneath a flat background for $P_{\rm miss} \geq 200$ MeV/c. At $E_{\rm miss} > 80$ MeV or $P_{\rm miss} > 200$ MeV/c, the cross section does not depend on $E_{\rm miss}$ and decreases only weakly with $P_{\rm miss}$. This flat cross section is similar to that seen in previous ^{12}C measurements and is due to multinucleon knockout.

We compared our results to single-particle knockout calculations by Kelly [21] and Ryckebusch [22–24] to determine how much of the observed continuum ($E_{\rm miss} >$ 20 MeV) cross section can be explained by $1s_{1/2}$-state knockout. Kelly [21] performed DWIA calculations using a relativized Schrödinger equation in which the dynamical enhancement of lower components of Dirac spinors is represented by an effective current operator [25]. He used the NLSH bound-state wave function [26] and the EDAIO optical potential [27]. These calculations accurately describe the $1p$-shell missing momentum distributions up to 340 MeV/c [20]. For the $1s_{1/2}$-state Kelly used a normalization factor of 0.73 and spread the cross section over missing energy using the Lorentzian parameterization of Mahaux [28]. At small $P_{\rm miss}$, where there is a clear peak at 40 MeV, this model describes the data well. At larger $P_{\rm miss}$, where there is no peak at 40 MeV, the DWIA cross section is much smaller than the measured cross section (see Figure 1). Relativistic DWIA calculations by other authors [29,30] show similar results. This confirms the attribution of the large missing momentum cross section to non-single-nucleon knockout.

Figure 1 also shows calculations by Ryckebusch *et al.* [22–24] using a non-relativistic single-nucleon knockout Hartree-Fock model which uses the same potential for both the ejectile and bound nucleons. Unlike DWIA, this approach conserves current at the one-body level, but it also requires much smaller normalization factors because it lacks a mechanism for diversion of flux from the single-nucleon knockout channel. At small missing momentum, this model describes both p-shell and s-shell cross sections well. As the missing momentum increases, it progressively overestimates the p-shell cross section. At $P_{\rm miss} > 200$ MeV/c, this model also predicts a nonexistent s-shell peak. The most important difference between the DWIA and HF single-nucleon knockout models is the absorptive potential; its omission increases the HF cross section for $P_{\rm miss} \sim 300$ MeV/c by an order of magnitude for both p-shell and s-shell.

Figure 1 also shows $(e,e'pn)$ and $(e,e'pp)$ contributions calculated by Ryckebusch *et al.* [31]. This calculation includes contributions mediated by pion-exchange currents, intermediate Δ creation and central and tensor short-range correlations. The flat cross section predicted by this calculation for $E_{\rm miss} > 50$ MeV is consistent with the data, although the magnitude is about half as large.

At high missing momenta, the cross section for $20 < E_{\rm miss} < 50$ MeV is not predicted by any of the models shown. This cross section could be due to the excitation of states with a complex structure in between the p- and s-shell.

Figure 2 presents the separated response functions for $\theta_{pq} = 0^\circ$ ($\langle P_{\rm miss} \rangle \approx 60$ MeV/c). The wide peak centered around $E_{\rm miss} \approx 40$ MeV in both R_L and R_T corresponds primarily to single-particle knockout from the $1s_{1/2}$-state. The difference between the transverse and longitudinal spectral functions $(S_T - S_L)$, which is expected to be zero for a free nucleon, is nonzero and appears to increase with $E_{\rm miss}$. The magnitude of $(S_T - S_L)$ measured here is consistent with the decrease in $(S_T - S_L)$ with Q^2 seen in the measurements of Ulmer *et al.* [2] at $Q^2 = 0.14$ (GeV/c)^2 and by Dutta *et al.* [10] at $Q^2 = 0.6$ and 1.8 (GeV/c)^2. This suggests that, in parallel kinematics, transverse non-single-nucleon knockout processes decrease with Q^2.

Figure 3 presents the separated response functions (R_{L+TT}[3], R_T and R_{LT}) for $|\theta_{pq}| = 8^\circ$ ($\langle P_{\rm miss} \rangle \approx 145$ MeV/c). The Mahaux parameterization does not reproduce the shape of R_L or of R_T as a function of missing energy. For $E_{\rm miss} < 35$ MeV, all calculated response functions underestimate the data. For $E_{\rm miss} > 50$ MeV, R_{L+TT} (which is mainly longitudinal because $\frac{V_{TT}}{V_L} R_{TT}$ is estimated to be only about 7% of R_L [21]) is consistent

[3] $R_{L+TT} \equiv R_L + \frac{V_{TT}}{V_L} R_{TT}$

with both zero and the calculations. R_T, on the other hand, remains nonzero to at least 60 MeV. This is consistent with the parallel kinematics results ($\theta_{pq} = 0$). R_T is also significantly larger than the DWIA calculation. R_{LT} is about twice as large as all three calculations over the entire range of $E_{\rm miss}$. R_{LT} is nonzero for $E_{\rm miss} > 50$ MeV, indicating that R_L is also nonzero in that range.

Figure 4 presents the separated response functions for $|\theta_{pq}| = 16^\circ$ ($\langle P_{\rm miss} \rangle \approx 280$ MeV/c). At this missing momentum, none of the response functions show a peak at $E_{\rm miss} \approx 40$ MeV where single-particle knockout from the $1s_{1/2}$-state is expected. R_{L+TT} is close to zero and the DWIA calculation. However, R_T and R_{LT} are much larger than the DWIA calculation. R_T is also much larger than R_{LT}. This indicates that the cross section is due to a predominantly transverse, non-single-nucleon knockout mechanism. The fact that R_{LT} is nonzero indicates that R_L, although too small to measure directly, is also nonzero.

To summarize, we have measured ^{16}O$(e,e'p)$ cross sections and response functions (R_L, R_T and R_{LT}) in quasielastic kinematics at $Q^2 = 0.8$ (GeV/c)^2 and $\omega = 439$ MeV for missing energies $25 < E_{\rm miss} < 120$ MeV at various missing momenta $P_{\rm miss} \leq 340$ MeV/c. For $25 < E_{\rm miss} < 50$ MeV and $P_{\rm miss} \approx 60$ MeV/c the reaction is dominated by single-nucleon knockout from the $1s_{1/2}$-state. $(S_T - S_L)$ is smaller than that measured at $Q^2 = 0.14$ [2] and $Q^2 = 0.6$ (GeV/c)^2, but larger than that measured at $Q^2 = 1.8$ (GeV/c)^2 [10]. This is consistent with the previous observation [10] that, at low $P_{\rm miss}$, non-single-nucleon knockout processes decrease with Q^2.

At higher missing momenta, the single-particle aspects are increasingly masked by more complicated states and processes. The cross section and the response functions no longer peak at the maximum of the s-shell (40 MeV). They no longer have the expected Lorentzian shape for s-shell knockout. For $P_{\rm miss} > 200$ MeV/c, the cross section and response functions are almost constant for $E_{\rm miss} > 25$ MeV. Theoretical calculations support these conclusions. DWIA calculations underestimate the cross section and response functions at $P_{\rm miss} > 200$ MeV/c by more than a factor of 10. This result is the opposite of the p-shell, where DWIA calculations describe the data well up to $P_{\rm miss} = 340$ MeV/c.

At larger missing energy, $80 < E_{\rm miss} < 120$ MeV, the cross section is almost constant with both missing energy and missing momentum. Two-nucleon knockout calculations, $(e,e'pp)$ plus $(e,e'pn)$, reproduce this constant behavior, and underestimate the cross section by only a factor of 2.

In conclusion, although the ^{16}O$(e,e'p)$ reaction at $E_{\rm miss} < 25$ MeV (1p-shell) is well described by single-nucleon DWIA calculations even at missing momenta much larger than the fermi momentum, this is not true for $E_{\rm miss} > 25$ MeV. In this case, the reaction is well described by single-nucleon knockout calculations only at low missing momentum ($P_{\rm miss} < 100$ MeV/c). At higher missing momenta, the single-particle aspects are increasingly masked by more complicated states and processes.

We acknowledge the outstanding support of the staff of the Accelerator and Physics Divisions at Jefferson Laboratory that this experiment successful. We thank Dr. J. Ryckebusch for providing theoretical calculations. We also thank Dr. J.M. Udias for providing us with the NLSH bound-state wave functions. This work was supported in part by the U.S. Department of Energy, the National Science Foundation, the Italian Istituto Nazionale di Fisica Nucleare (INFN), the French Atomic Energy Commission and National Center of Scientific Research, and the Natural Sciences and Engineering Research Council of Canada.

[1] J.J. Kelly, Adv. Nucl. Phys. **23**, ed. by J.W. Negele and E. Vogt, 75 (1996).
[2] P.E. Ulmer *et al.*, Phys. Rev. Lett. **59**, 2259 (1987).
[3] R. Lourie *et al.*, Phys. Rev. Lett. **56**, 2364 (1986).
[4] L. Weinstein *et al.*, Phys. Rev. Lett. **64**, 1646 (1990).
[5] J.H. Morrison, Phys. Rev. **C59**, 221 (1999).
[6] T. de Forest, Nucl. Phys. A **392,** 232 (1983).
[7] T. de Forest, Ann. Phys **45**, 365 (1967).
[8] J.B.J.M. Lanen *et al.*, Phys. Rev. Lett. **64**, 2250 (1990).
[9] G. van der Steenhoven *et al.*, Nucl. Phys. **A480**, 547 (1988).
[10] D. Dutta, Ph.D. thesis, Northwestern University, 1999 (unpublished).
[11] J. Ryckebusch *et al.*, Nucl. Phys. **A624**, 581 (1997).
[12] A. Gil *et al.*, Nucl. Phys. **A627**, 599 (1997).
[13] T. Takaki, Phys. Rev. **C39**, 359 (1989).
[14] H. Muther *et al.*, Phys. Rev. **C49**, R17 (1994).
[15] A. Saha, W. Bertozzi, R.W. Lourie, and L.B. Weinstein, Jefferson Laboratory Proposal 89-003, 1989; K.G. Fissum, MIT-LNS Internal Report #02, 1997.
[16] F. Garibaldi *et al.*, Nucl. Instrum. Methods **A314,** 1 (1992).
[17] www.jlab.org/Hall-A/equipment/HRS.html
[18] N. Liyanage, Ph.D. thesis, MIT, 1999 (unpublished).
[19] E. Quint, Ph.D. thesis, University of Amsterdam, 1988 (unpublished).
[20] J. Gao *et al.*, Phys. Rev. Lett. **84**, 3265 (2000); J. Gao, Ph.D. thesis, MIT, 1999 (unpublished).
[21] J.J. Kelly, Phys. Rev. **C60**, 044609 (1999).
[22] J. Ryckebusch *et al.*, Nucl. Phys. **A476**, 237 (1988).
[23] J. Ryckebusch *et al.*, Nucl. Phys. **A503**, 694 (1989).
[24] V. Van der Sluys *et al.*, Phys. Rev. **C55** 1982 (1997).
[25] M. Hedayati-Poor, J.I. Johansson, and H.S. Sherif, Phys. Rev. **C51**, 2044 (1995)
[26] M.M. Sharma, M.A. Nagarajan, and P. Ring, Phys. Lett. **B312**, 377 (1993).
[27] E.D. Cooper, S. Hama, B.C. Clark, and R.L. Mercer, Phys. Rev. **C47**, 297 (1993).

[28] J.P. Jeukenne and C. Mahaux, Nucl. Phys. **A394**, 445 (1983).
[29] A. Picklesimer, J. W. van Orden, and S. J. Wallace, Phys. Rev. **C 32**, 1312 (1985).
[30] J. M. Udías, J. A. Caballero, E. M. de Guerra, J. E. Amaro, and T. W. Donnelly, Phys. Rev. Lett. **83**, 5451 (1999).
[31] S. Janssen, J. Ryckebusch, D. Debruyne and W. Van Nespen, Nucl. Phys. **A672**, 285 (2000).

$E_{\rm beam}$ (GeV)	θ_e (°)	θ_{pq} (°)
0.843	100.7	0, 8, 16
1.643	37.2	0, ±8
2.442	23.4	0, ±2.5, ±8, ±16, ±20

TABLE I. Experimental Kinematics.

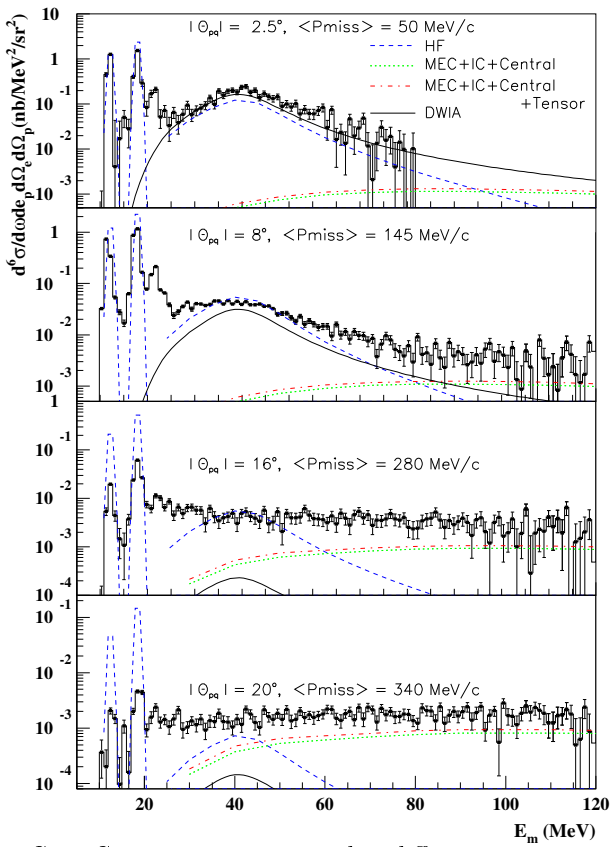

FIG. 1. Cross sections measured at different outgoing proton angles as a function of missing energy. The curves show the $1s_{1/2}$-state single-particle strength calculated by Kelly (solid curve) and by Ryckebusch (dashed curve), folded with the Lorentzian parameterization of Mahaux. The dotted line shows the Ryckebusch *et al.* calculations of the $(e,e'pn)$ and $(e,e'pp)$ contributions to $(e,e'p)$ including meson-exchange currents (MEC), intermediate Δ creation (IC) and central correlations, while the dot-dashed line also includes tensor correlations.

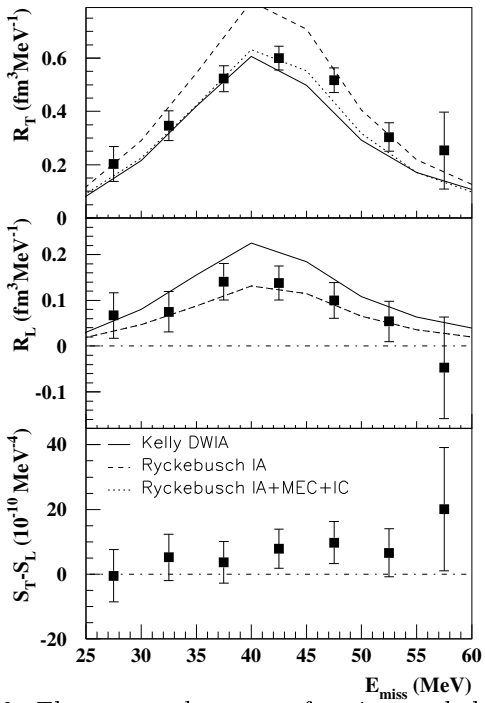

FIG. 2. The separated response functions and the difference of the longitudinal and transverse spectral functions for $|\theta_{pq}| = 0°$ ($\langle P_{\rm miss}\rangle \approx 60$ MeV/c). The calculations have been binned in the same manner as the data.

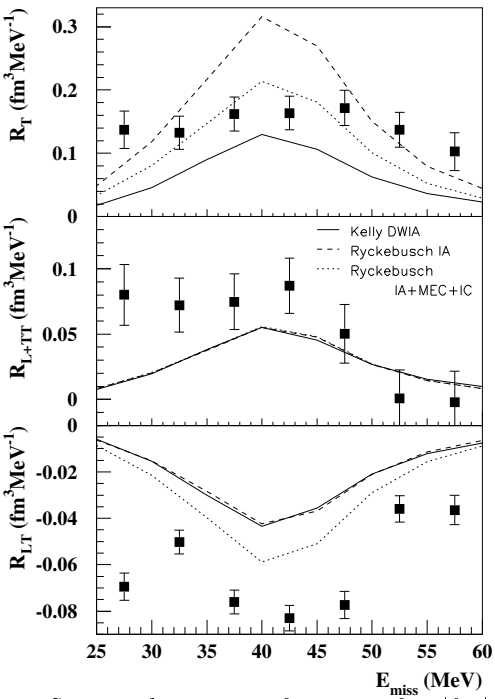

FIG. 3. Separated response functions for $|\theta_{pq}| = 8°$ ($\langle P_{\rm miss}\rangle^{average} \approx 145$ MeV/c).

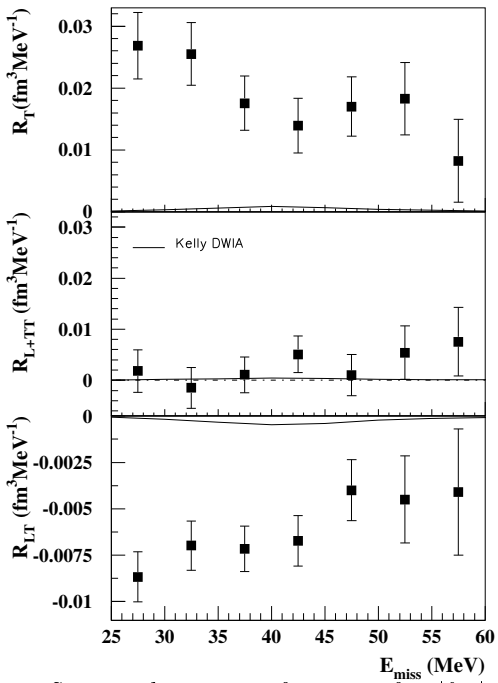

FIG. 4. Separated response functions for $|\theta_{pq}| = 16°$ ($\langle P_{\rm miss}\rangle \approx 280$ MeV/c).